https://erjm.journals.ekb.eg
ISSN: 1110-1180

DOI: ---------

ERJ
Engineering Research Journal
Faculty of Engineering
Menoufia University

Wavelet-Based Differential Protection Scheme for Power Transformers

Amira M. Dahman[1], Adel A. Abou El-Ela[1], Ragab A. El Sehiemy[2]

[1] *Faculty of Engineering, Electrical Engineering Department, Menoufiya University, gypt*
[2] *Electrical Engineering Department, Faculty of Engineering, Kafrelsheikh University, Egypt.*
(Corresponding author: amira.mohamed4880@sh-eng.menofia.edu.eg)

ABSTRACT
This paper presents a new wavelet-based scheme as a differential protection algorithm for power transformers. The eliminated method deals with enhanced discrete wavelet transform with detail and approximate coefficients and implement them to energy equations as a new wavelet based technique. The proposed scheme processing is applied to a various variety of transient conditions and successfully verified for transformer protection. Transformers are subjected to many abnormal events against normal operation condition such as magnetization inrush condition, external fault condition and interturn winding faults against turn to earth faults and turn to turn faults also. Simulation results are obtained and approved to sensitivity and reliability of the proposed scheme in transformer protection against all fault cases and also in fault identification and localization. However, the discussed approach also simulate fault under variety of conditions such as different fault resistances, different fault ratio and in case of external fault. The simulated system applies a CT saturation condition and also examines the selected approach against this fault type with different fault resistances against both 3-phase and single phase fault conditions. The simulation fault cases approve the sensitivity and accuracy of the selected scheme even the simplicity of the proposed scheme enhances the advantages and features toward transformer protection.

Keywords: *wavelet transform; internal winding faults; magnetizing inrush; transformer protection.*

1. Introduction

The choice of protection schemes to power systems are subjected to many difficulties. The most important equipment in the power system plays an important role in the selection of the most suitable protection scheme. Differential protection is the most widely used scheme in presence of transformer in power systems. However, the investigation of differential relay suffers many problems that cause mal operation due to various phenomena according to the nonlinearities in transformer core [1], [2].

The faults related to transformer protection are worthy classified into two main categories, external faults and internal faults. External faults happen outside transformer windings where internal faults are related to winding failures such as turn to earth faults and turn to turn faults. Magnetizing inrush current is a reliable discriminative case needed to be analyzed and discriminated from internal fault cases.

So, many protection scheme associated with differential protection are applied to transformer protection. Such as second harmonic technique [3]. But, it was reported that this technique falls blew in the presence of inrush magnetizing current produced in the case of reenergizing of the power transformer or after fault removement which has high harmonic content causing the relay to mal operate[4]. Avoiding these limitations, processing techniques have been presented recently, such as:

Volt and flux restraints [5], inductance based methods [6], wavelet transform [7-9], restricted earth fault protection based on wavelet transform technique [7], artificial intelligence [8], support vector machines (SVM) [4,10], artificial neural network techniques [11], fuzzy logic control technique [9, 12], S-transform based method [13], and negative sequence approach [14-16].

Relevant works in this area have already focused on internal fault models and have depended on identifying the section of fault in transmission lines while the impact of transformer was not proposed. The comparison of negative sequence protection algorithm but it was noticed that the algorithm is not applied for all cases of internal faults and also cannot distinguish inrush current and turn to turn fault when occur simultaneously.

This work presents a discrete wavelet transform based method for power transformer differential protection scheme. The proposed method deals with the operating wavelet energy coefficients that are obtained using the extracted currents from both end measurements as shown in Fig.1. The extracted currents are analyzed using MATLAB program and with suitable processing, the energy coefficient features are extracted and calculated. Once, the energy coefficients exceed a predefined threshold, a fault is detected and type of fault is cleared to take the suitable action of the relay.

The following sections describe the carried work in this paper: the next section introduces the proposed wavelet transform technique. Then, system model is presented. The simulation results based on the proposed scheme and conclusions are drawn in the last two working sections.

2. Proposed Wavelet Transform Method

Figure(2) depicts the flow chart of the proposed discrete wavelet transform based on differential energy coefficients. The proposed method is mentioned in detail as following.

2.1 Differential Current

First of all, the measured current, taken out of the two end measurements of the simulated system on ATP program, is applied to MATLAB program with the selected sampled frequency (10 kHz). Then, the sampled current is calculated in pu system to simplify calculations and clear any errors.

The differential current is calculated related to the primary and secondary transformer winding currents which are given by the classical form:

$$I_d = I_{HV} - I_{LV} \qquad (1)$$

The calculated differential current is subjected to the suitable filters to get rid of any noise or undesired frequencies.

2.2 Discrete Wavelet Transform (DWT)

Furthermore, the sampled differential current is subjected to DWT to be analyzed and identified to compute details and approximate coefficients. These sampled coefficients are modified and applied to the relay. The following equations give approximation (A1) coefficients and detail (D1) coefficients, respectively. DWT provides indexes in both time and frequency domains for analyzing transient signals. In contrast, the selection of the processed mother wavelet plays an important role in fault identification and transient state features differ from mother wavelet to another. The proposed method select db1 as the main mother wavelet for fault analyzing and fault identification[17].

$$A1[k] = \sum_{n=-\infty}^{\infty} X[n] * L[n-2k] \qquad (2)$$

$$D1[k] = \sum_{n=-\infty}^{\infty} X[n] * h[n-2k] \qquad (3)$$

Where $X[n]$ is the sampled signal, k represents the translation interval, $L[n]$ and h $[n]$ are scaling and wavelet filters [18].

2.3 Differential energy coefficients

Consequently, the output processed signal coefficients for both detail and approximate coefficients are applied to energy equations to compute the absolute sum of detail energy coefficient and approximate energy coefficient. Then, the differential energy are computed according to Eqn. (9). In normal operation the three phase absolute values are closely the same while in fault conditions the absolute levels show difference values.

2.4 The threshold definition

The energy of a discrete signal $I_i(n)$ is calculated as follow Eqn. (8). The differential energy factor calculated at Eqn. (9) shows the severity and the kind of relation. This factor is between 0 and 1.

3. System Under Study

Simulation is performed with ATP program performing a 3-ph power system with two ends supplies [19]. A two winding power transformer rated at 32MVA, 115/22 kV, YNd11 configuration and Usc=32% as shown in Figure(1) . the performed system is supplied with nonlinear models of standard CTs rated at CT1, CT3=50/1 and CT2, CT4=200/1. The power transformer is simulated by support of BCTRAN subroutine to involve internal winding faults. The extracted features of ATP and BCTRAN subroutine are processed in MATLAB with sampling frequency 10kHz.

Involving CT in power system simulation improves the reliability and enhance the sensitivity of relay to overcome the limitations related to CT implementation in the system. CTs can produce unexpected and unpredictable effects when external faults occur, causing undesired currents leading to maloperation of the protection relay such cases are called CT saturation due to nonlinear characteristics of CTs as tabulated in Table (1).

$$\beta = (abs(DET(I_{diffA}) - DET(I_{diffB}) - DET(I_{diffc}))) * \Psi \qquad (4)$$

$$Q = \min(DET_i) \qquad (5)$$

$$\omega = avr(DET_i)/1.25 \qquad (6)$$

$$E_i = \sum_{j=1}^{n} I_i^2(j) \quad (7)$$

$$T_i = \min(abs(I_i)) \quad \lambda_i = \max(abs(I_i)) \quad (8)$$

$$DIFFenergy_i = ((E_i - T_i^2)/(\lambda_i^2 - T_i^2)) \quad (9)$$

where, **Ψ** is varied between 0.2-0.35, DETi refers to the detail coefficient for one of the three phases as i is the selected phase (A, B or C) and APPROi refers to the approximation coefficient for one of the three phases as i is the selected phase (A, B or C).

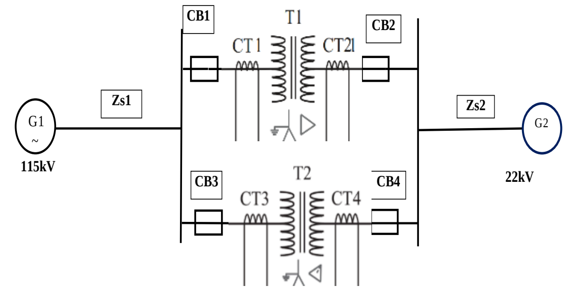

Figure 1- Schematic diagram of the HV/LV system under study.

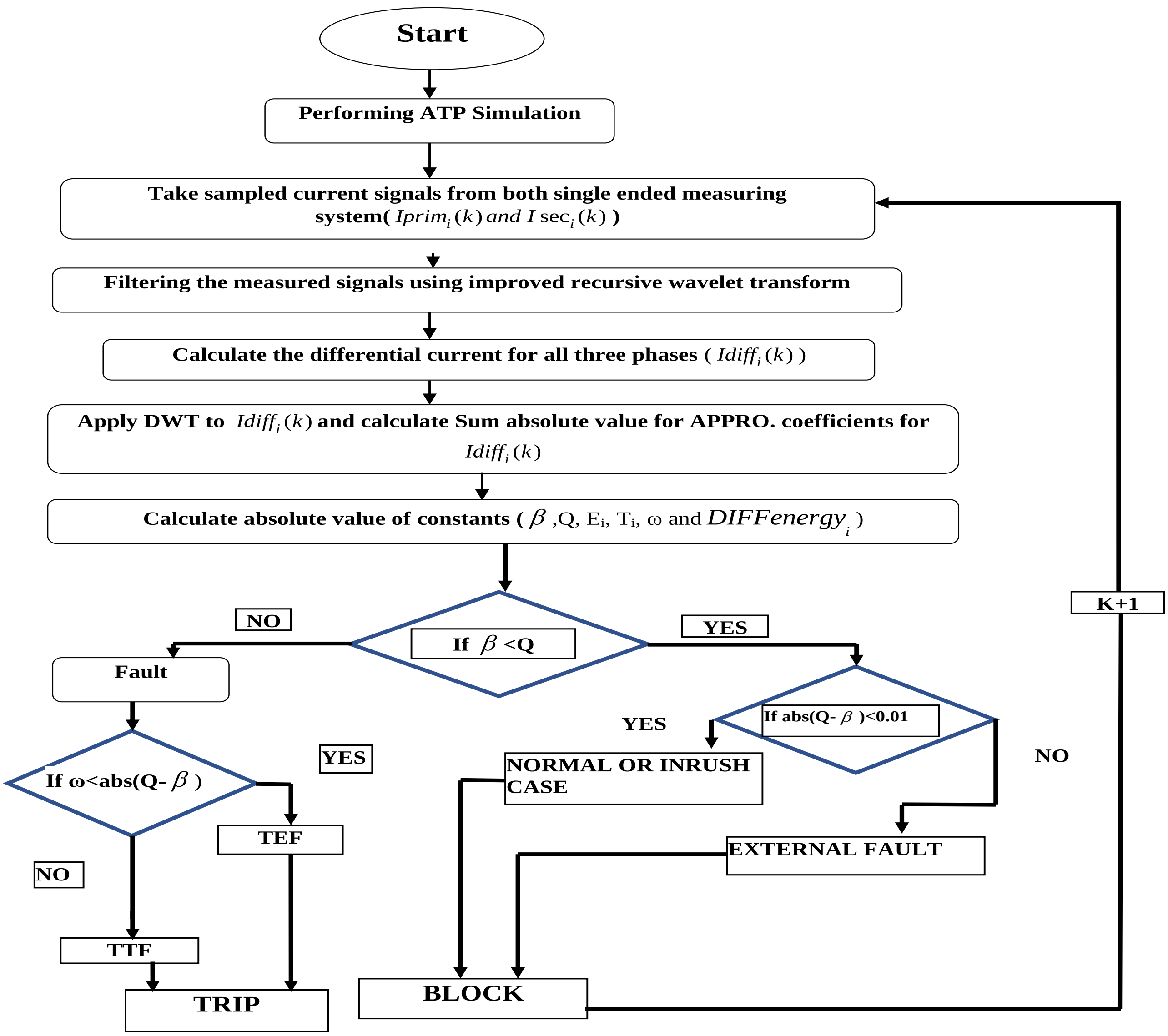

Figure 2- The proposed scheme flow chart

4. Simulation Results

All exact current signals taken out of ATP and current processed signals analyzed using MATLAB are firstly computed in normal and stable condition. Then, the transient condition are applied to show the differences from normal operation and take the most sensitive action of the relay. External faults depict high differences from stable operation but the relay should give a block operation not a trip one. Also here, magnetizing inrush condition also should block the relay. While, internal faults (turn to earth and turn to turn) should give a trip action.

Moreover, the healthy matrices drawn using BCTRAN subroutine lead to two 6*6 matrices give the [R] and [L] of each winding and mutual inductances between windings, while in fault condition applied to internal windings of transformer, the size of matrices turns to 7*7 and 8*8 in case of turn to earth faults and turn to turn faults, respectively.

In this section, the results of simulated system applying the sequence of the flow chart in Fig. 2 after MATLAB program processing are evaluated. The studied cases are normal operation, inrush case, an inrush case with applied internal turn to earth and turn to turn fault conditions, an external fault condition, internal fault conditions (turn to earth and turn to turn) and finally external fault condition in CT saturation effect presence.

4.1 Protection Against Inrush Condition

Both normal condition and inrush current case are reported in all researches as normal operation of power transformers that means no trip action should be taken out of the protection relay.

Hence, the proposed scheme is evaluated against the simulated inrush case and also, evolving both cases of internal faults. Figure (3) gives the simulated results. As shown in Figure (3) the total energy of detail coefficient for all the three phases are closely the same. However, beta constant is lower than the predefined threshold which means no trip action of the proposed relay. Figure (4) gives the same inrush case but followed by a turn to earth fault condition with highly differences in total energy coefficients. Moreover, the results depict a deviation between the 3-phases with highly amplitude of phase A (the faulty phase) leading to maximize the beta constant against the predefined threshold that make the proposed scheme identify fault occurrence.

Table (2) tabulates the results representing the success of proposed method in discriminating inrush condition between internal fault case.

4.2 Protection Against External Fault Condition

Here, the relay must be tested against external faults and the proposed scheme should be able to identify fault type and discriminate between internal and external faults. At Figure(5), a 3-ph external fault near transformer point is applied to the protection system. The results show that almost the three phases are stable and produce the same levels of detail and approximate coefficients handling the beta constant blew the predefined threshold with a block relaying signal.

However, in Figure(6), a single line to neutral external fault is applied to the system. At faulty winding phase A gives almost high levels of detail and approximate energy coefficients but the conclusion at differential energy coefficients is almost stable at the three phases and blew the predefined threshold. As expected, the external fault is defined and discriminated against internal fault conditions.

Although the relay has showed a high sensitivity in identifying internal faults and in discrimination between internal and external faults, the implementation of CTs at power systems may produce unexpected currents especially when external faults lead the CTs enter the saturation zone. The effect of CT saturation could mal operate the relay and send a false trip signal. External fault is simulated under CT saturation effect at faulty wye winding of the transformer. Here, at single line to ground fault at phase A at wye winding as shown in Figure(7), the proposed scheme results depict no increasement in the beta constant against the predefined threshold as the differential energy coefficients of all three phases are almost the same.

The sensitivity of the proposed scheme is enhanced after testing CTs saturation effect on the protection system. Table (3) proposes the results for a 3-phase external fault and a single line to ground external fault. Also, Table (3) tabulates a 3-phase external fault ang a single line to ground external fault against CT saturation with conclusion, the external fault is handled as no faulty case.

4.3 Protection Against Internal Fault Condition

The internal fault condition results are then discussed in Figure(8) and Figure(9), while the fault is applied to phase A at wye winding of transformer connection with fault ratio 60% of total turns and fault resistance 45Ω. In Figure(8), the differential current shows a high increase in phase A (the faulty phase) compared to phase B and phase C and almost fifty times the rated current that needs a fast action of the relay. Also, the proposed algorithm analysis presents the levels reached by detail and approximate energy coefficients which result in an increment in beta constant against the predefined threshold.

In Figure(9) turn to turn case, applied to phase A at wye winding of transformer connection with fault ratio 40% of total turns, depicts an abnormal operation against normal operation with lightly smaller values of the absolute sum of energy coefficients and the predefined differential energy coefficient. The calculated constants are verified in TTF (turn to turn fault) case resulting in abnormal conclusion make the relay take a trip action as the flow chart steps define fault condition.

Some other results cases of internal fault condition are depicted in Table (4) with the trip action of the proposed relay. Table (3) describes the variation of fault parameters such as fault ratio and fault resistance to enhance the sensitivity and reliability of the proposed scheme.

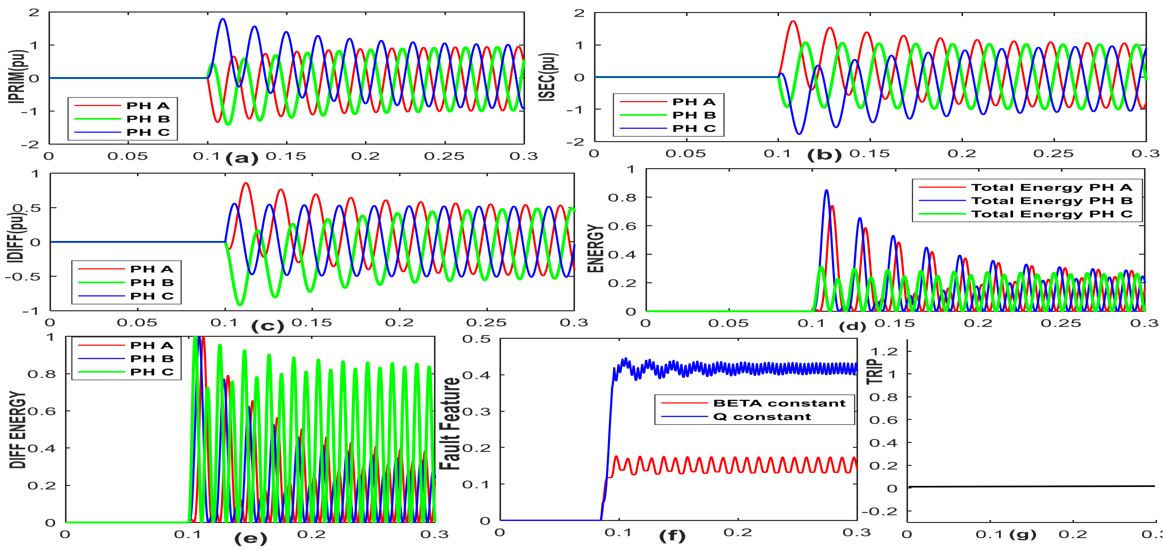

Figure3- Magnetizing inrush condition a) primary currents b) secondary currents c) phases differential current d) phases total Energy e) phases differential energy coefficients f) threshold vs. beta constant g) final relay decision.

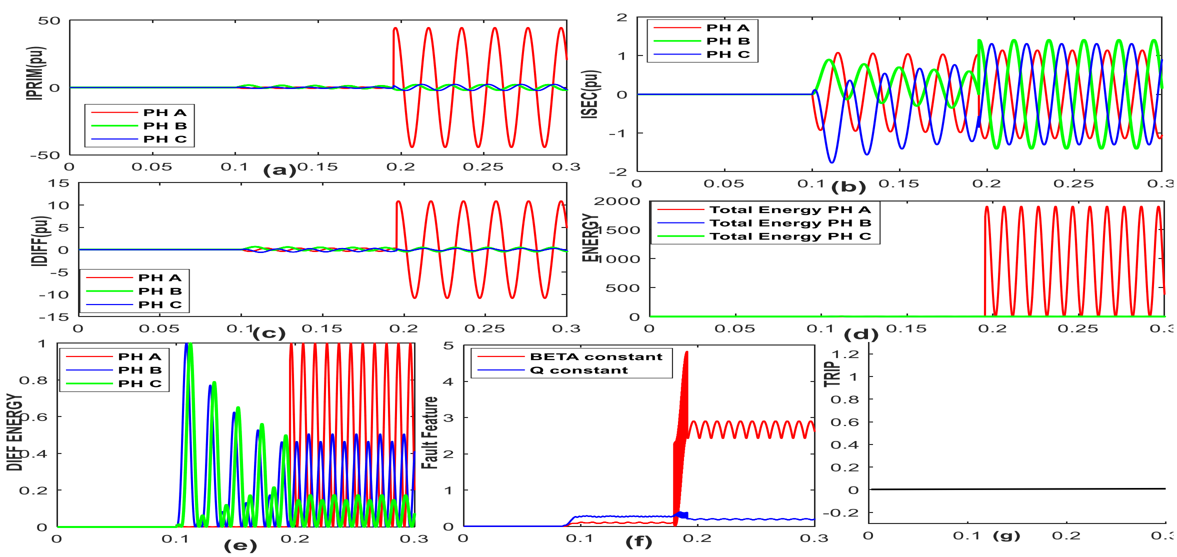

Figure 4- Inrush then TEF(turn to earth fault) at 30% of phase A of primary winding at fault resistance 70Ω case a) primary currents b) secondary currents c) phases differential current d) phases total Energy e) phases differential energy coefficients f) threshold vs. beta constant g) final relay decision.

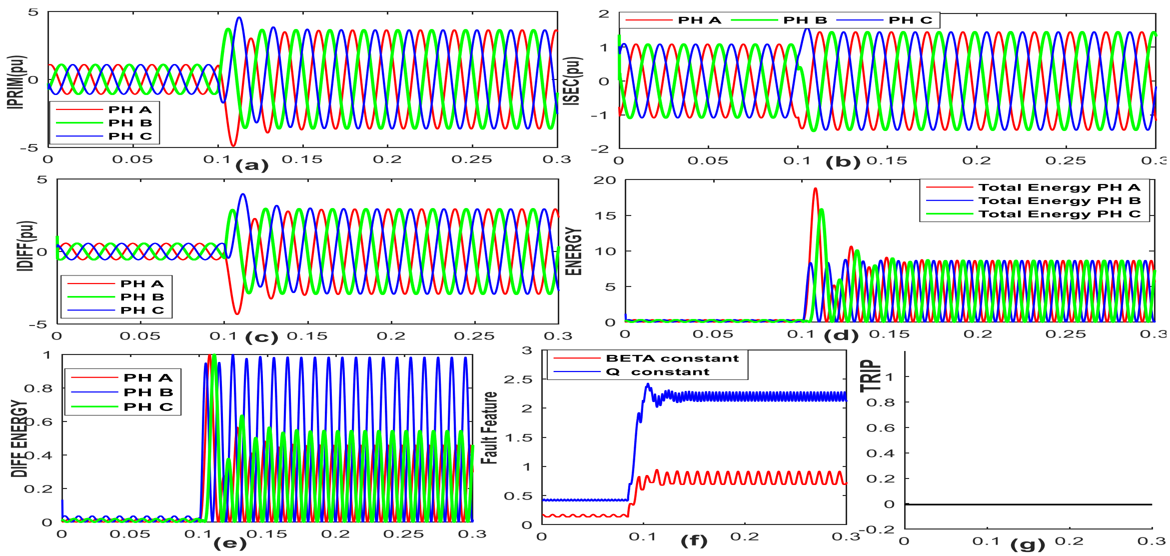

Figure 5- External 3-PH fault with fault resistance 0.001Ω case a) primary currents b) secondary currents c) phases differential current d) phases total Energy e) phases differential energy coefficients f) threshold vs. beta constant g) final relay decision.

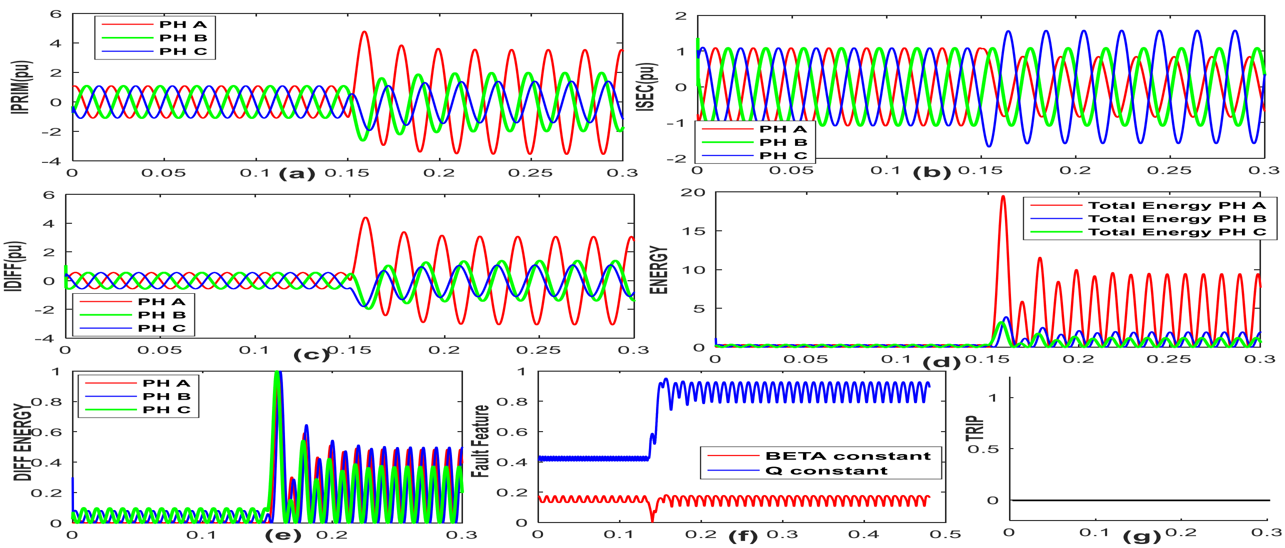

Figure 6- External A-G fault with fault resistance 65Ω case a) primary currents b) secondary currents c) phases differential current d) phases total Energy e) phases differential energy coefficients f) threshold vs. beta constant g) final relay decision.

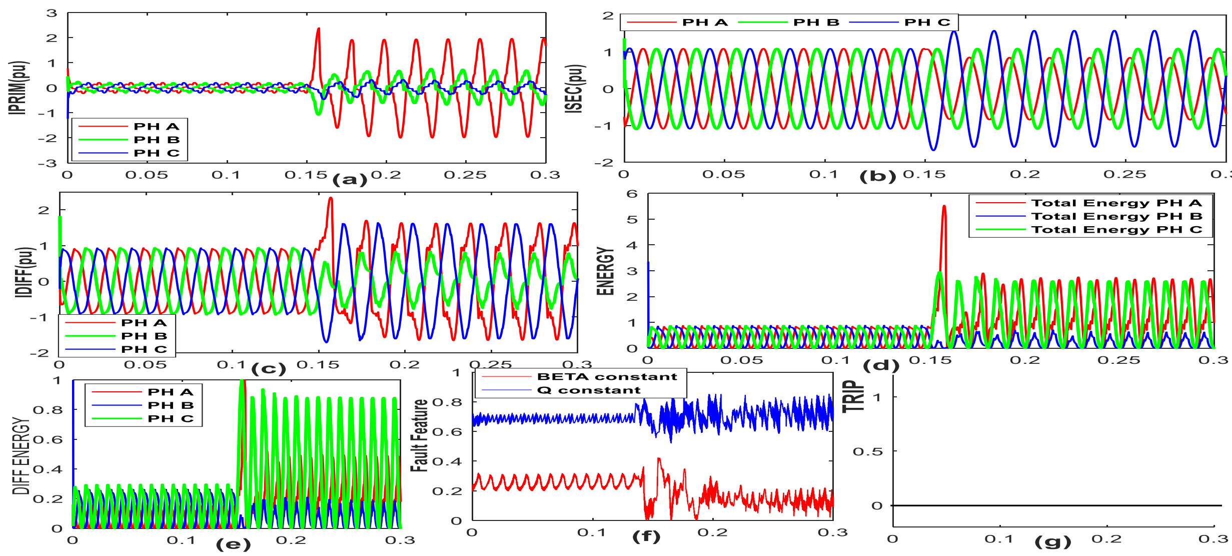

Figure 7- External A-G fault combined with CT saturation with fault resistance 0.001Ω case a) primary currents b) secondary currents c) phases differential current d) phases total Energy e) phases differential energy coefficients f) threshold vs. beta constant g) final relay decision.

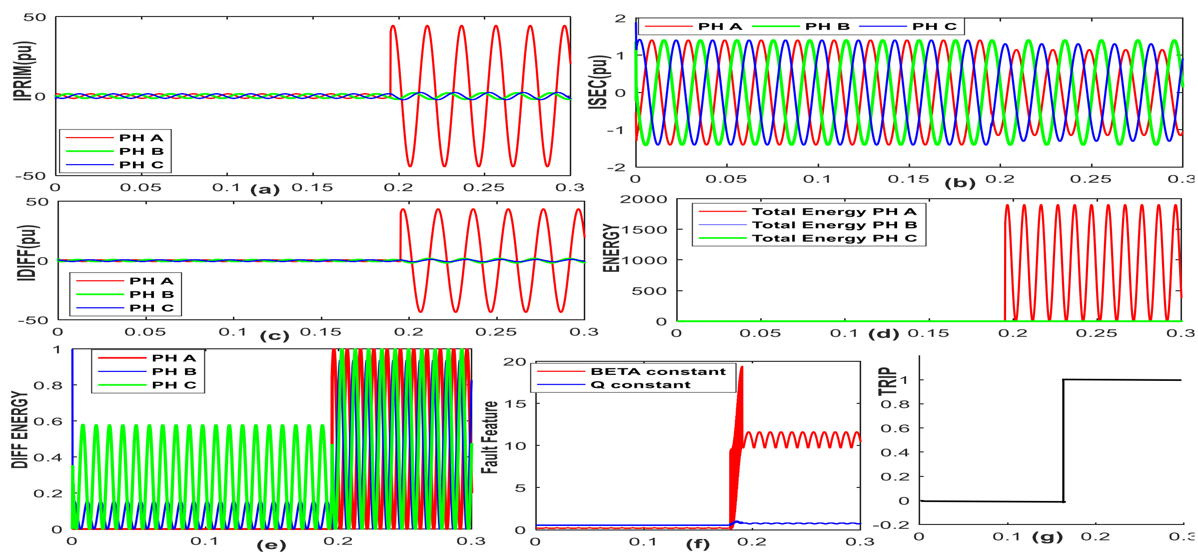

Figure 8- Internal TEF case at 40% of phase A of primary winding with fault resistance 5 Ω a) primary currents b) secondary currents c) phases differential current d) phases total Energy e) phases differential energy coefficients f) threshold vs. beta constant g) final relay decision.

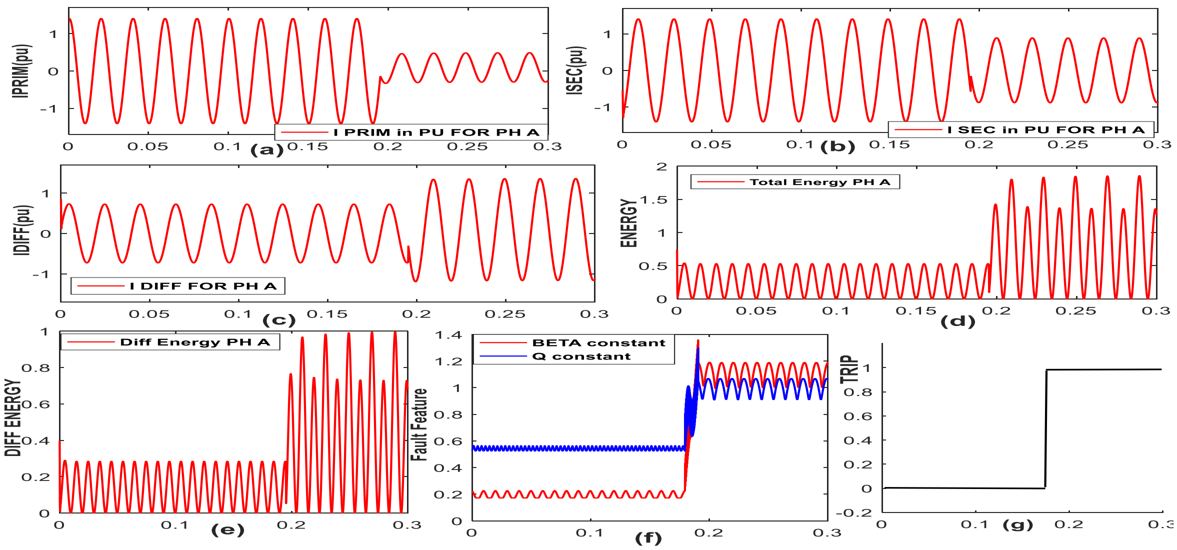

Figure 9- Internal TTF(turn to turn fault) case at 40% of phase A turns of primary winding a) primary currents b) secondary currents c) phases differential current d) phases total Energy e) phases differential energy coefficients f) threshold vs. beta constant g) final relay decision.

Table 1- CT1 Saturation non linear characteristics

Current (A)	Flux Linked (Wb-T)	Current (A)	Flux Linked (Wb-T)
-36.825	-94.9129412	11.66125	70.3270588
-18.4125	-93.769412	16.57125	78.9035294
-6.1375	-90.917694118	24.55	85.7647059
-1.2275	-88.0517647	36.21125	90.3388235
2.148125	-81.1905882	56.465	93.7694118
4.05075	-68.6117647	98.2	97.2
7.365	49.1717647	135.025	97.7717647

Table 2– Inrush cases

Fault type	RF Ω	Fault ratio	Fault-Identification Index						Final Relay Decision
			DET A	DET B	DET C	APPRO A	APPRO B	APPRO C	
Healthy	---	------	0.01028	0.01235	0.01187	21.094	17.6613	18.4634	Block
INRUSH	---	------	0.00592	0.0062	0.00515	9.29544	8.84927	10.5499	Block
Inrush then TEF	45Ω	20%	38.911	0.07666	0.02052	72538.3	113.269	36.5247	Block
Inrush then TTF	---	15%	0.05064	0.28092	0.03462	72.9562	460.822	46.5286	Block

Table 3– External fault studied cases

Fault type	*RF (Ω)*	*Fault-Identification Index*						*Final Decision*
		DET A	*DET B*	*DET C*	*APPRO A*	*APPRO B*	*APPRO C*	
Healthy	---	0.01028	0.01235	0.01187	21.094	17.6613	18.4634	Block
External 3-Phase fault	0.001Ω	0.19534	0.16764	0.20053	299.055	344.989	290.435	Block
	12Ω	0.19534	0.16764	0.20053	299.055	344.989	290.435	Block
	Ω 150	0.19534	0.16764	0.20053	299.055	344.989	290.435	Block
External A-G fault	Ω 0.01	0.22053	0.04686	0.02659	315.068	62.5966	42.6143	Block
	Ω 10	0.19122	0.04246	0.02339	282.761	56.6025	40.0549	Block
	Ω 100	0.042	0.01647	0.00958	78.1972	22.1008	19.0363	Block
External A-G- fault with CT saturation	0.001 Ω	0.08783	0.0229	0.04903	89.7395	16.4837	97.9402	Block
	Ω 5	0.09173	0.02698	0.0495	85.4755	18.1582	99.6815	Block
	45Ω	0.0838	0.0179	0.0519	54.6982	19.8971	99.2907	Block
	Ω 300	0.03242	0.02171	0.03139	39.1472	32.4538	57.5004	Block
External 3-phase fault with CT saturation	0.001 Ω	0.10902	0.12672	0.18333	121.953	123.915	110.95	Block
	Ω 12	0.10901	0.12672	0.18331	121.952	123.912	110.948	Block
	Ω 150	0.10902	0.12674	0.18336	121.95	123.91	110.946	Block

Table 4–Normal case and internal fault studied conditions

Fault type	RF (Ω)	Fault ratio	Fault-Identification Index						Final Relay Decision
			APPRO A	APPRO B	APPRO C	DET A	DET B	DET C	
Healthy	---	------	21.094	17.6613	18.4634	0.01028	0.01235	0.01187	BLOCK
TEF	Ω 0.5	a=0.2&b=0.8	72546.6	110.467	35.2465	38.9177	0.07795	0.02107	TRIP
	45Ω	a=0.6&b=0.4	72514.5	105.769	33.4074	38.8994	0.07445	0.01961	TRIP
	150Ω	a=0.9&b=0.1	72525	107.308	34	38.9054	0.07559	0.02008	TRIP
TTF		a=0.15$b=0.4$c=0.45	62.4636	318.114	170.397	0.03811	0.23935	0.12917	TRIP
		a=0.15$b=0.65$c=0.2	56.2636	410.816	253.339	0.04232	0.30794	0.18888	TRIP
		=a b=0.05$c=0.35$0.6	64.8163	129.657	32.8907	0.04542	0.09553	0.02354	TRIP

5. Conclusions

This paper has improved a wavelet-based fault identification scheme. The proposed fault identification approach depends on current signals after processing simulation on MATLAB. The proposed scheme has been simulated on 32MVA power transformer with two end measurements, the extracted currents have been evaluated depending on a selected constants which are exactly able to identify fault type. Even fault conditions are examined against different fault resistances, different fault ratio and different fault location. Finally, the simulation results are evaluated and tabulated with final conclusion, the external fault is handled as no faulty case and the relay take a trip action in case of internal fault cases showing the success and the sensitivity of the approved wavelet-based technique in transformer protection.

References

[1] E. Ali, A. Helal, H. Desouki, K. Shebl, S. Abdelkader, and O. P. Malik, "Power transformer differential protection using current and voltage ratios," Electr. Power Syst. Res., vol. 154, pp. 140–150, 2018, doi: 10.1016/j.epsr.2017.08.026.

[2] D. Bejmert, M. Kereit, F. Mieske, W. Rebizant, K. Solak, and A. Wiszniewski, "Power transformer differential protection with integral approach," Int. J. Electr. Power Energy Syst., vol. 118, no. September 2019, p. 105859, 2020, doi: 10.1016/j.ijepes.2020.105859.

[3] P. Liu, D. Chen, Y. Guo, O. P. Malik, and G. S. Hope, "Improved operation of differential protection of power transformers for internal faults," IEEE Trans. Power Deliv., vol. 7, no. 4, 1992, doi: 10.1109/61.156994.

[4] E. Ali, O. P. Malik, A. Knight, S. Abdelkader, A. Helal, and H. Desouki, "Ratios-based universal differential protection algorithm for power transformer," Electr. Power Syst. Res., vol. 186, p. 106383, Sep. 2020, doi: 10.1016/J.EPSR.2020.106383.

[5] M. Mostafaei and F. Haghjoo, "Flux-based turn-to-turn fault protection for power transformers," IET Gener. Transm. Distrib., vol. 10, no. 5, 2016, doi: 10.1049/iet-gtd.2015.0738.

[6] K. Inagaki et al., "Digital protection method for power transformers based on an equivalent circuit composed of inverse inductance," IEEE Trans. Power Deliv., vol. 3, no. 4, 1988, doi: 10.1109/61.193949.

[7] M. N. O. Aires, R. P. Medeiros, F. B. Costa, K. M. Silva, J. J. Chavez, and M. Popov, "A w avelet-based restricted earth-fault power transformer differential protection," Electr. Power Syst. Res., vol. 196, no. April, p. 107246, 2021, doi: 10.1016/j.epsr.2021.107246.

[8] L. D. Simões, H. J. D. Costa, M. N. O. Aires, R. P. Medeiros, F. B. Costa, and A. S. Bretas, "A power transformer differential protection based onsupport vector machine and wavelet transform," Electr. Power Syst. Res., vol. 197, no. April, 2021, doi: 10.1016/j.epsr.2021.107297.

[9] M. Jamil, R. Singh, and S. K. Sharma, "Fault identification in electrical power distribution system using combined discrete wavelet transform and fuzzy logic," J. Electr. Syst. Inf. Technol., vol. 2, no. 2, 2015, doi: 10.1016/j.jesit.2015.03.015.

[10] J. Zupan, "Introduction to Artificial Neural Network (ANN) Methods : What They Are and How to Use Them *.," no. September, pp. 327–352, 1994.

[11] Z. Li, Z. Jiao, and A. He, "K nowledge-based ar tificial neural network for power transformer protection," IET Gener. Transm. Distrib., vol. 14, no. 24, pp. 5816–5822, 2020, doi: 10.1049/iet-gtd.2020.0542.

[12] R. Umre and P. V. T. Barhate, "Power transformer protection using Clark's trans-formation and fuzzy logic," pp. 34–39, 2014.

[13] A. Behvandi, S. G. Seifossadat, and A. Saffarian, "A new method for discrimination of internal fault from other transient states in power transformer using Clarke's transform and modified hyperbolic S-transform," Electr. Power Syst. Res., vol. 178, no. April 2019, 2020, doi: 10.1016/j.epsr.2019.106023.

[14] L. M. R. Oliveira and A. J. M. Cardoso, "Comparing Power Transformer Turn-to-Turn Faults Protection Methods: Negative Sequence Component Versus Space-Vector Algorithms," IEEE Trans. Ind. Appl., vol. 53, no. 3, 2017, doi: 10.1109/TIA.2016.2613506.

[15] D. Zacharias and R. Gokaraju, "Prototype of a Negative-Sequence Turn-to-Turn Fault Detection Scheme for Transformers," IEEE Trans. Power Deliv., vol. 31, no. 1, 2016, doi: 10.110 9/TPWRD.2015.2483524.

[16] M. Pan, C. Gu, Z. Yu, J. Shan, B. Liu, and D. Zheng, "Fault detection and protection of UHV transmission line based on negative sequence impedance angle," IOP Conf. Ser. Earth Environ. Sci., vol. 598, no. 1, 2020, doi: 10.1088/1755-1315/598/1/012100.

[17] B. Noshad, M. Razaz, and S. G. Seifossadat, "A new algorithm based on Clarke's Transform and Discrete Wavelet Transform for the differential protection of three-phase power transformers considering the ultra-saturation phenomenon," Electr. Power Syst. Res., vol. 110, pp. 9–24, 2014, doi: 10.1016/j.epsr.2014.01.001.

[18] M. I. Zaki, R. A. El-Sehiemy, G. M. Amer, and F. M. Abo El Enin, "An investigated reactive power measurements-based fault-identification scheme for teed transmission lines," Meas. J. Int. Meas. Confed., vol. 136, 2019, doi: 10.1016/j.measurement.2018.12.068.

[19] Association of Tennis Professionals, "The 2021 ATP ® Official Rulebook," 2021, Available online: https://www.atptour.com/en/corporate/rulebook.